Figures and figure supplements

MiRNA-128 regulates the proliferation and neurogenesis of neural precursors by targeting PCM1 in the developing cortex
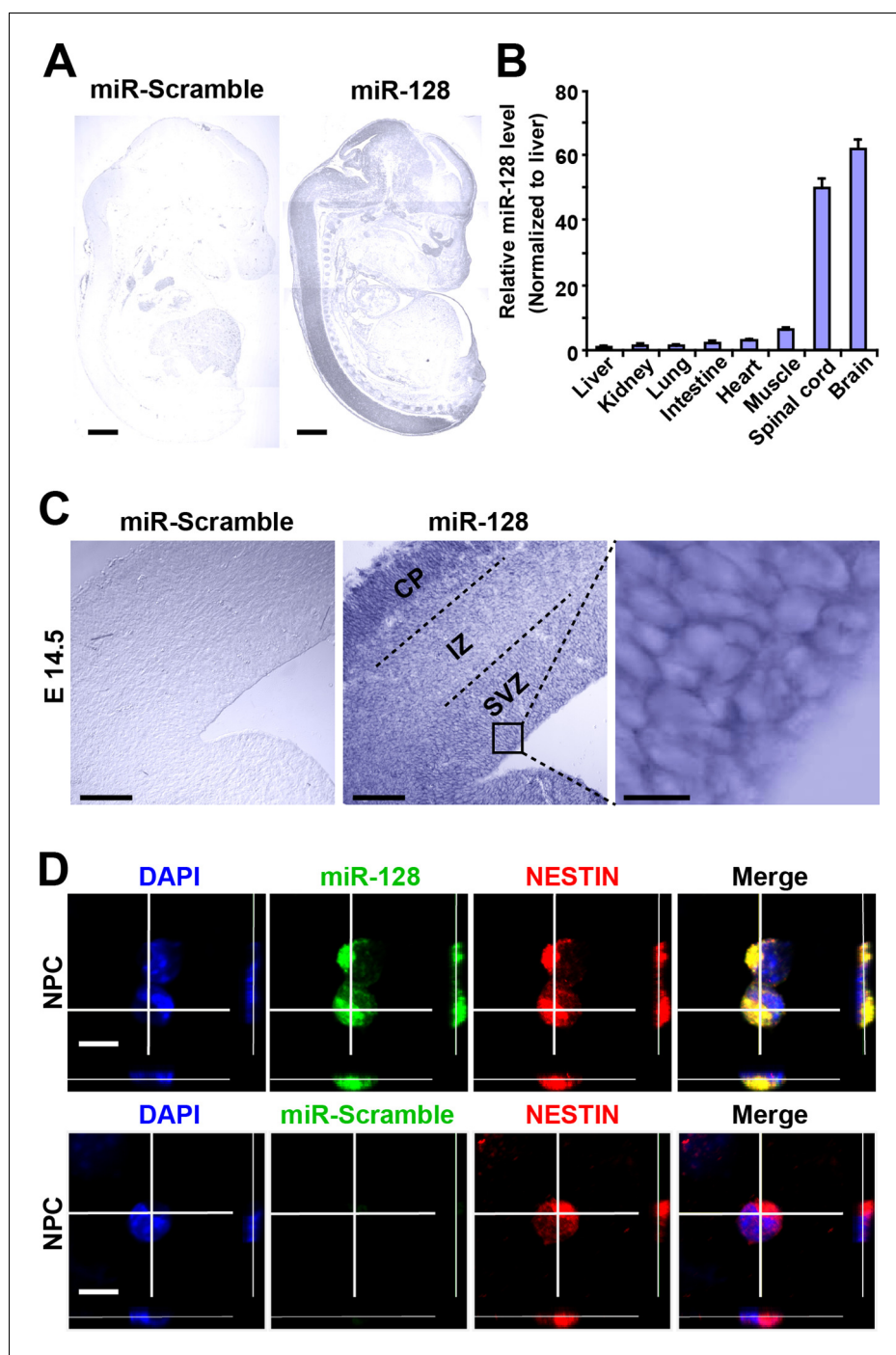
Wei Zhang *et al*

Figure 1. miR-128 expression in the developing cerebral cortex. (A) ISH was performed in an E17.5 mouse embryo with a miR-128 LNA detection probe. A sagittal section shows that miR-128 is expressed in the CNS. The left-side section was probed with a miR scramble control. Scale bars, 1 mm. (B) Real-time qPCR analyses of miR-128 from various tissues at E17.5, showing that miR-128 is highly expressed in the brain and spinal cord. miR-128 expression was measured and normalized to that of U6 and is shown relative to the liver expression level. The values represent the mean ± s.d. (n = 3). (C) miR-128 expression in the cortex. ISH was performed in an E14.5 mouse embryo brain coronal section with a miR-128 LNA detection probe. The left-side section was probed with a miR scramble control. Scale bars, 50 μm, and 5 μm in the higher magnification image (right-most panel). (D) miR-128 expression in NPCs in vitro. miR-128 LNA in situ hybridization followed by immunofluorescence analysis of the neural stem cell marker NESTIN in NPCs. DAPI staining indicates the location of cell nuclei. Scale bars, 10 μm.
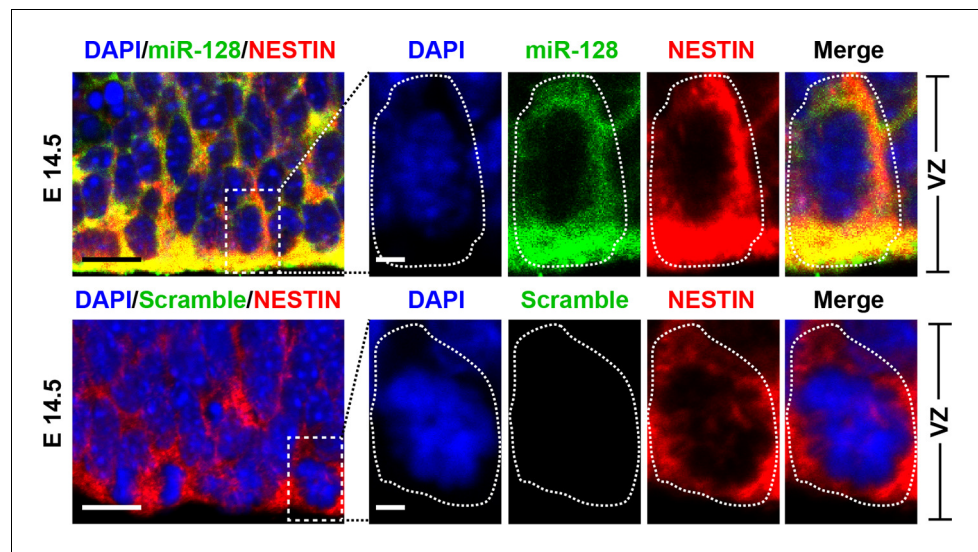DOI: 10.7554/eLife.11324.003

Figure 1—figure supplement 1. miR-128 expression in the developing CNS. miR-128 expression in the NPCs of the VZ at E14.5. miR-128 LNA in situ hybridization followed by immunofluorescence analysis of the neural stem cell marker NESTIN on E14.5 mouse embryo brain coronal sections. The micrographs in the bottom panels show slices probed with a miR scramble control. White dotted line outlines a single cell within the VZ. DAPI staining indicates the location of cell nuclei. Scale bars, 5 μm in left-most panel, 2 μm in all other panels.
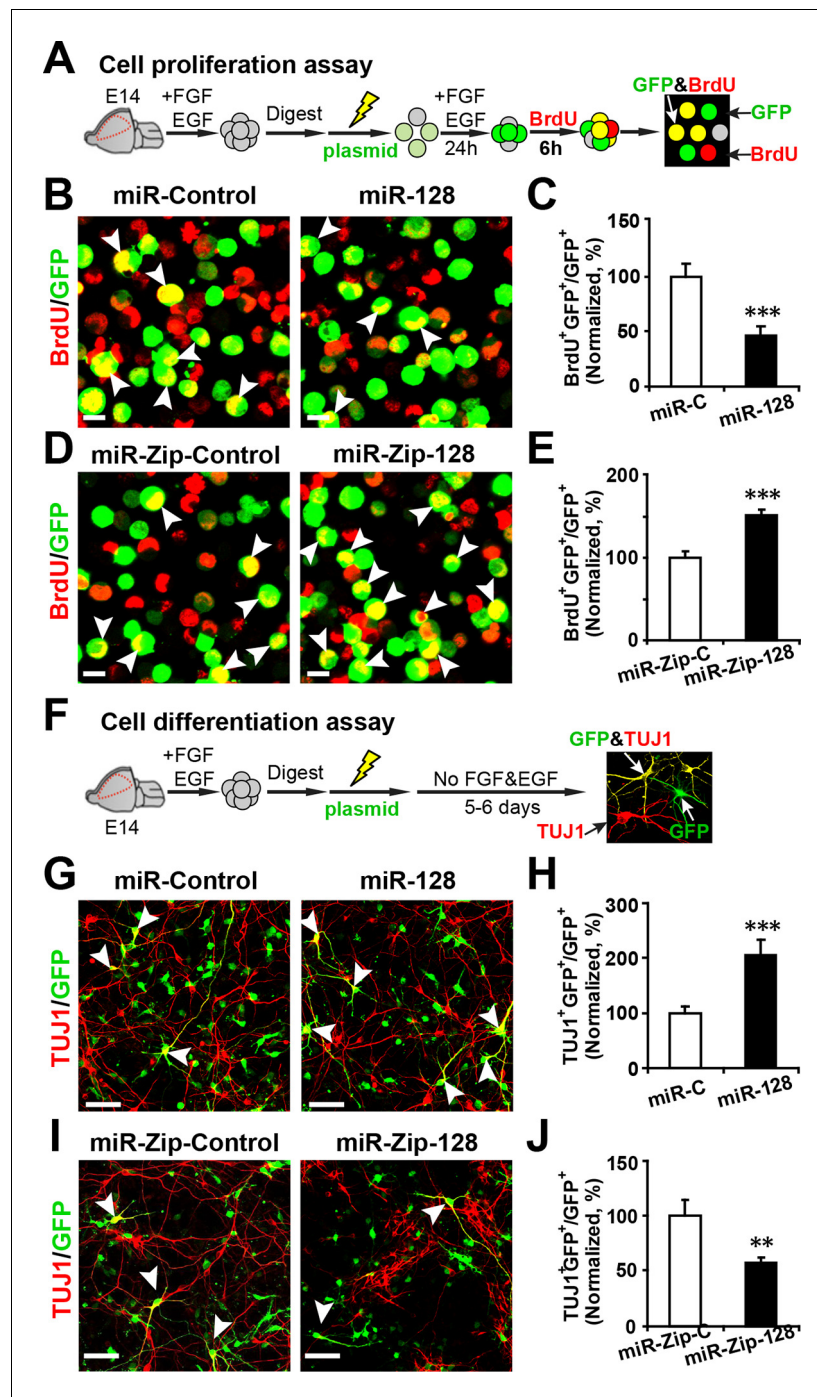DOI: 10.7554/eLife.11324.004

Figure 2. miR-128 modulates the proliferation and differentiation of NPCs in vitro. (**A**) Schematic representation of the cell proliferation assay procedures. (**B-E**) Ectopic expression of miR-128 decreases proliferation, while that of miR-Zip-128 increases NPC proliferation. NPCs were electroporated with the indicated plasmids and pulse-labeled with BrdU for 6 hr. NPCs were immunostained with an antibody against BrdU. The arrowheads indicate BrdU and GFP double-positive cells. Scale bars, 10 μm. Quantification of the number of GFP-BrdU double-positive cells relative to the total number of GFP-positive cells (**C, E**). (**F**) Schematic representation of the cell differentiation assay procedures. (**G-J**) Ectopic expression of miR-128 increases neurogenesis, while that of miR-Zip-128 decreases the neurogenesis of NPCs. NPCs were electroporated with the indicated plasmids and immunostained with antibodies against TUJ1. The arrowheads indicate TUJ1$^+$GFP$^+$ cells. Scale bars, 50 μm. Quantification of the number of the GFP-TUJ1 double-positive cells relative to the number of GFP-positive cells (**H, J**). More than 1500 GFP-positive cells were counted for each condition. At least three sets of independent experiments were

Figure 2 continued on next page

Figure 2 continued

performed. The values represent the mean ± s.d. (n = 3). Student's *t*-test, differences were considered significant at ***$p<0.001$ and **$p<0.01$.
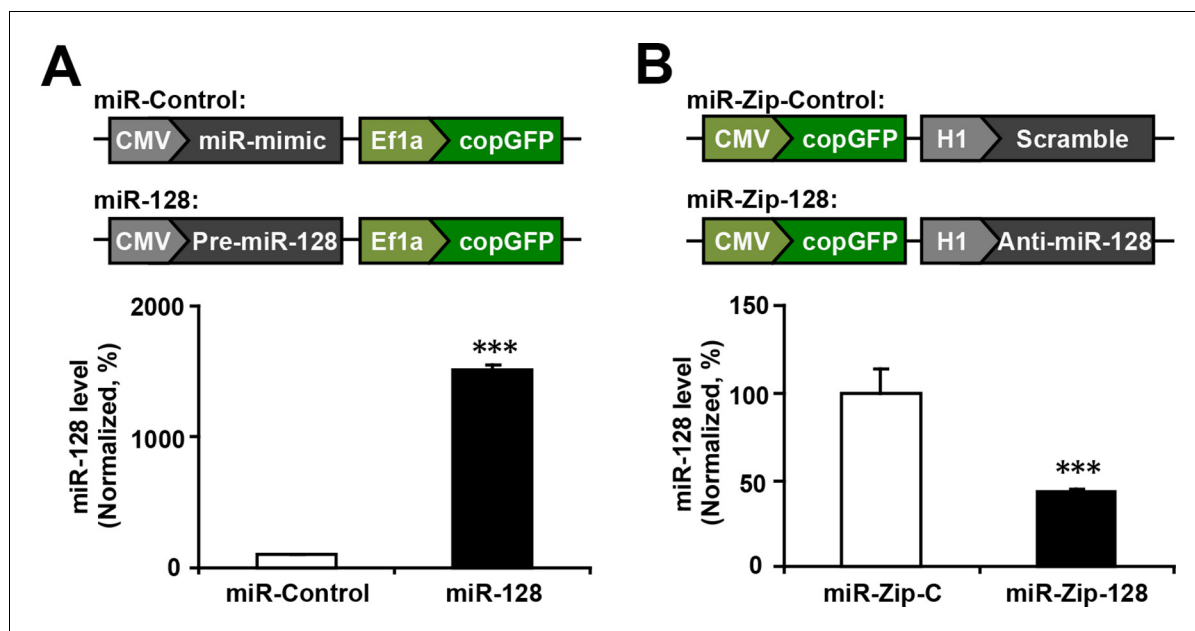
Figure 2—figure supplement 1. miR-128 overexpression and miR-128 knockdown constructs and their expression efficiency. (A) Premature miR-128-1 (pre-miR-128) was cloned into a dual expression construct. The corresponding control construct contained a random miR mimic sequence. (B) qPCR quantification of miR-128 levels in NPCs following transfection with the miR-128 constructs. (C) A shRNA sequence targeting mature miR-128 (anti-miR-128) was cloned into a dual expression construct. The corresponding control construct contained a scrambled shRNA sequence. (D) qPCR quantification of miR-128 levels in NPCs following transfection with the miR-Zip-128 constructs. The values represent the mean ± s.d. (n = 3). Student's *t*-test, differences were considered significant at ***p<0.001.
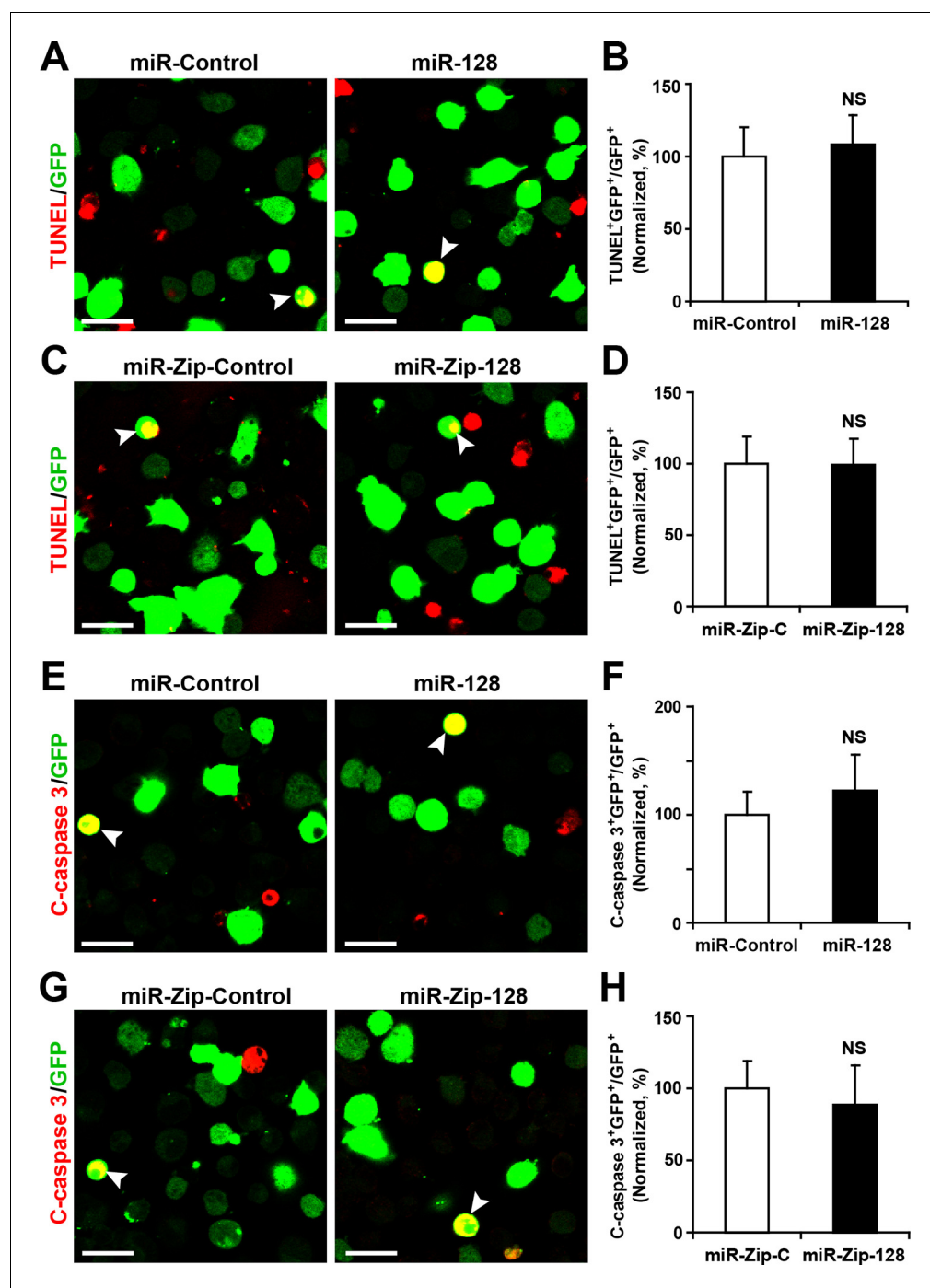DOI: 10.7554/eLife.11324.006

Figure 2—figure supplement 2. miR-128 overexpression and knockdown does not affect NPC apoptosis. (A-D) Ectopic expression of miR-128 and miR-Zip-128 does not affect TUNEL staining. Quantification of the number of GFP-TUNEL double-positive cells relative to the total number of GFP-positive cells (B, D). (E-H) Ectopic expression of miR-128 and miR-Zip-128 does not affect cleaved caspase-3 (C-caspase 3) staining. Scale bars, 20 μm. Quantification of the number of GFP-C-caspase 3 double-positive cells relative to the total number of GFP-positive cells (B, D). More than 1500 GFP-positive cells were counted for each condition. At least three sets of independent experiments were performed. The values represent the mean ± s.d. (n = 3). Student's t-test, differences were considered significant at $*p < 0.05$.
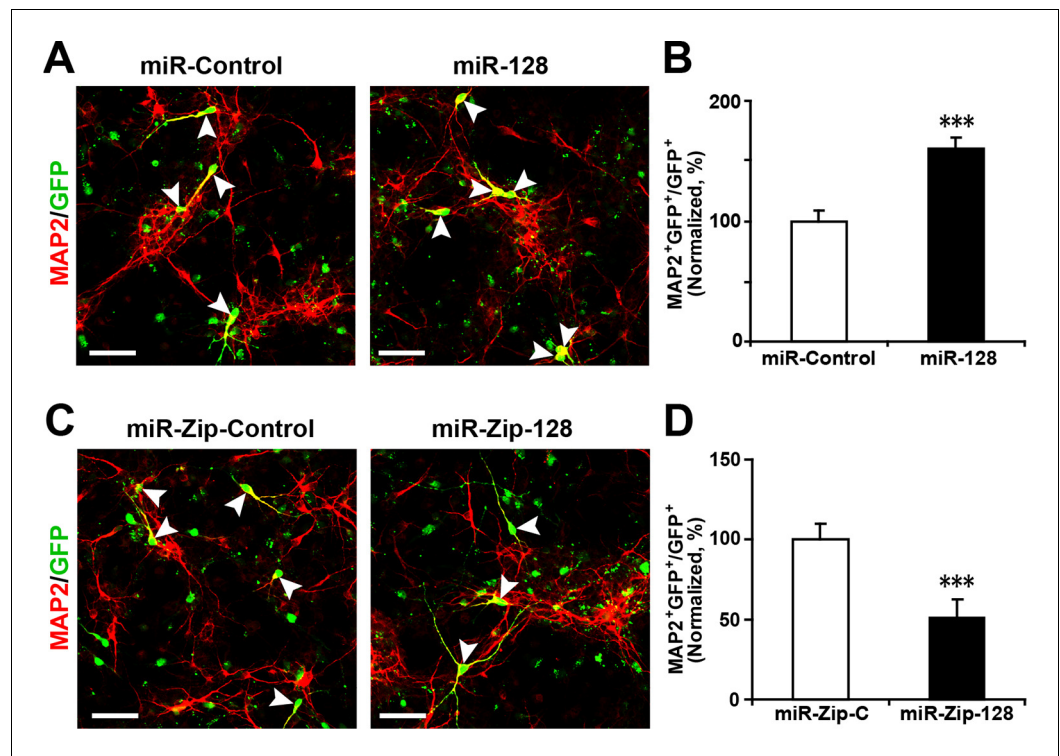
DOI: 10.7554/eLife.11324.007

Figure 2—figure supplement 3. Ectopic expression of miR-128 increases neurogenesis, while that of miR-Zip-128 decreases neurogenesis. (A-D) NPCs were electroporated with the indicated plasmids and immunostained with antibodies against MAP2. The arrowheads indicate MAP2$^+$GFP$^+$ cells. Scale bars, 50 μm. Quantification of the number of GFP-MAP2 double-positive cells relative to the number of GFP-positive cells (B, D). More than 1500 GFP-positive cells were counted for each condition. At least three sets of independent experiments were performed. The values represent the mean ± s.d. (n = 3). Student's *t*-test, differences were considered significant at ***p<0.001.
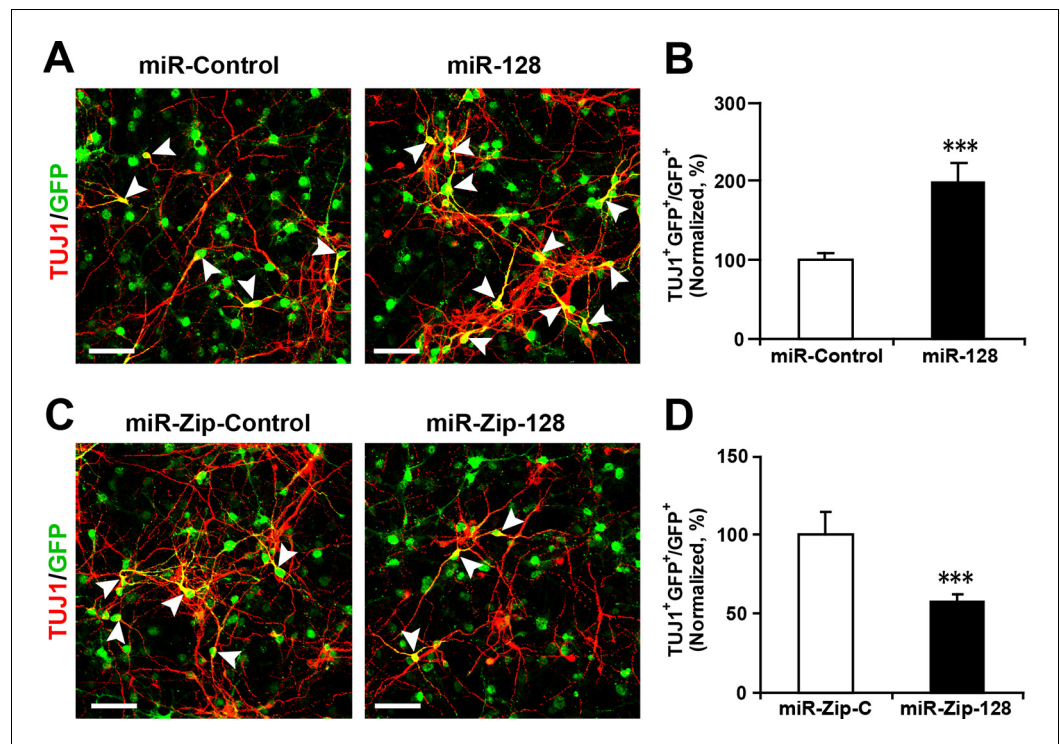
DOI: 10.7554/eLife.11324.008

Figure 2—figure supplement 4. Lentivirus-mediated transduction of miR-128 and miR-Zip-128 increases and decreases neurogenesis, respectively. (**A-D**) NPCs were transduced with lentiviruses carrying the indicated plasmids and immunostained with antibodies against TUJ1. The arrowheads indicate TUJ1$^+$GFP$^+$ cells. Scale bars, 50 µm. Quantification of the number of GFP-TUJ1 double-positive cells relative to the number of GFP-positive cells (**B, D**). More than 1500 GFP-positive cells were counted for each condition. At least three sets of independent experiments were performed. The values represent the mean ± s.d. (n = 3). Student's t-test, differences were considered significant at ***p<0.001.
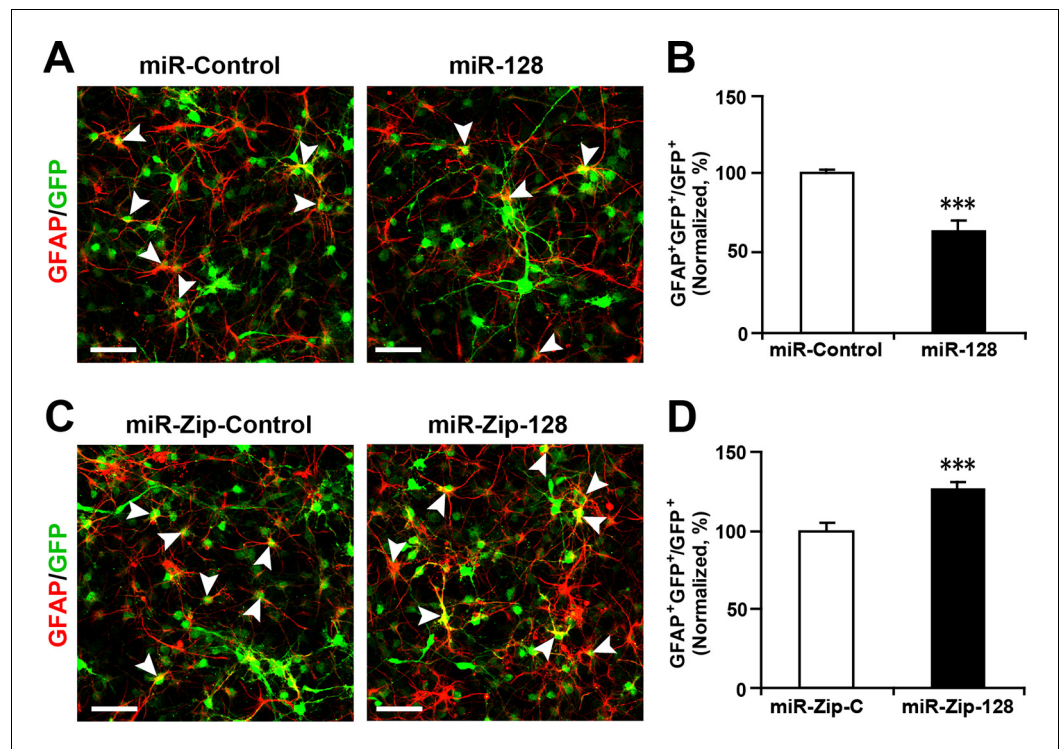DOI: 10.7554/eLife.11324.009

Figure 2—figure supplement 5. Ectopic expression of miR-128 decreases gliogenesis, while that of miR-Zip-128 increases gliogenesis. (A-D) NPCs were transduced with lentiviruses carrying the indicated plasmids and immunostained with antibodies against GFAP. The arrowheads indicate GFAP$^+$GFP$^+$ cells. Scale bars, 50 µm. Quantification of the number of GFP-GFAP double-positive cells relative to the number of GFP-positive cells (B, D). More than 1500 GFP-positive cells were counted for each condition. At least three sets of independent experiments were performed. The values represent the mean ± s.d. (n = 3). Student's t-test, differences were considered significant at ***p<0.001.
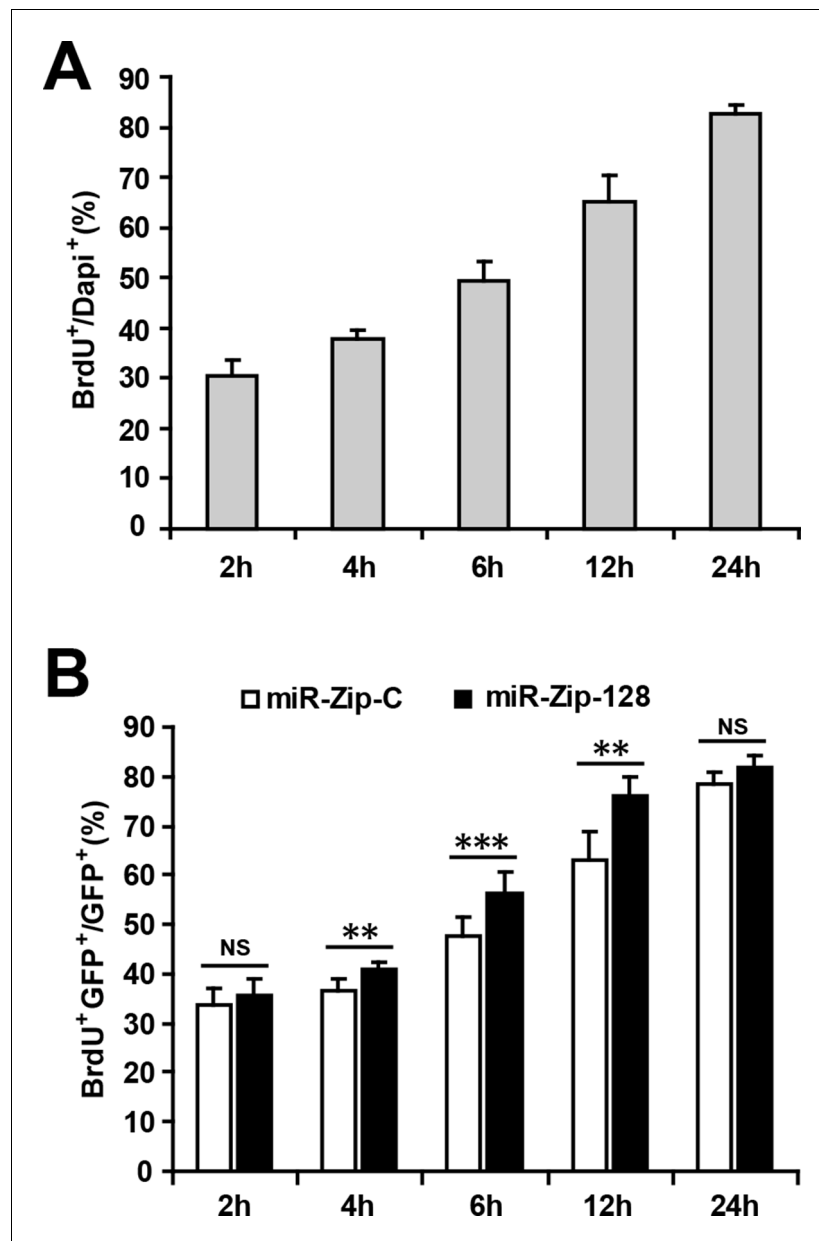DOI: 10.7554/eLife.11324.010

Figure 2—figure supplement 6. Optimizing the duration of BrdU pulse labeling for in vitro NPC proliferation assay. (A) NPCs were pulsed with BrdU for the indicated duration before fixation. Quantification of BrdU-positive cells over total DAPI-positive cells. (B) Following electroporation with either miR-128-ZIP or the control constructs NPCs were pulsed with BrdU for the indicated duration. Quantification of BrdU- GFP-double-positive cells over GFP-positive cells shows that after 4 hr of BrdU exposure, NPCs electroporated with miR-128-ZIP show significantly increased BrdU incorporation compared to control. At least 1500 cells were counted for each condition. The values represent the means ± s.d. (n = 3). Student's t-test, differences were considered significant at ***p<0.001, **p<0.01.
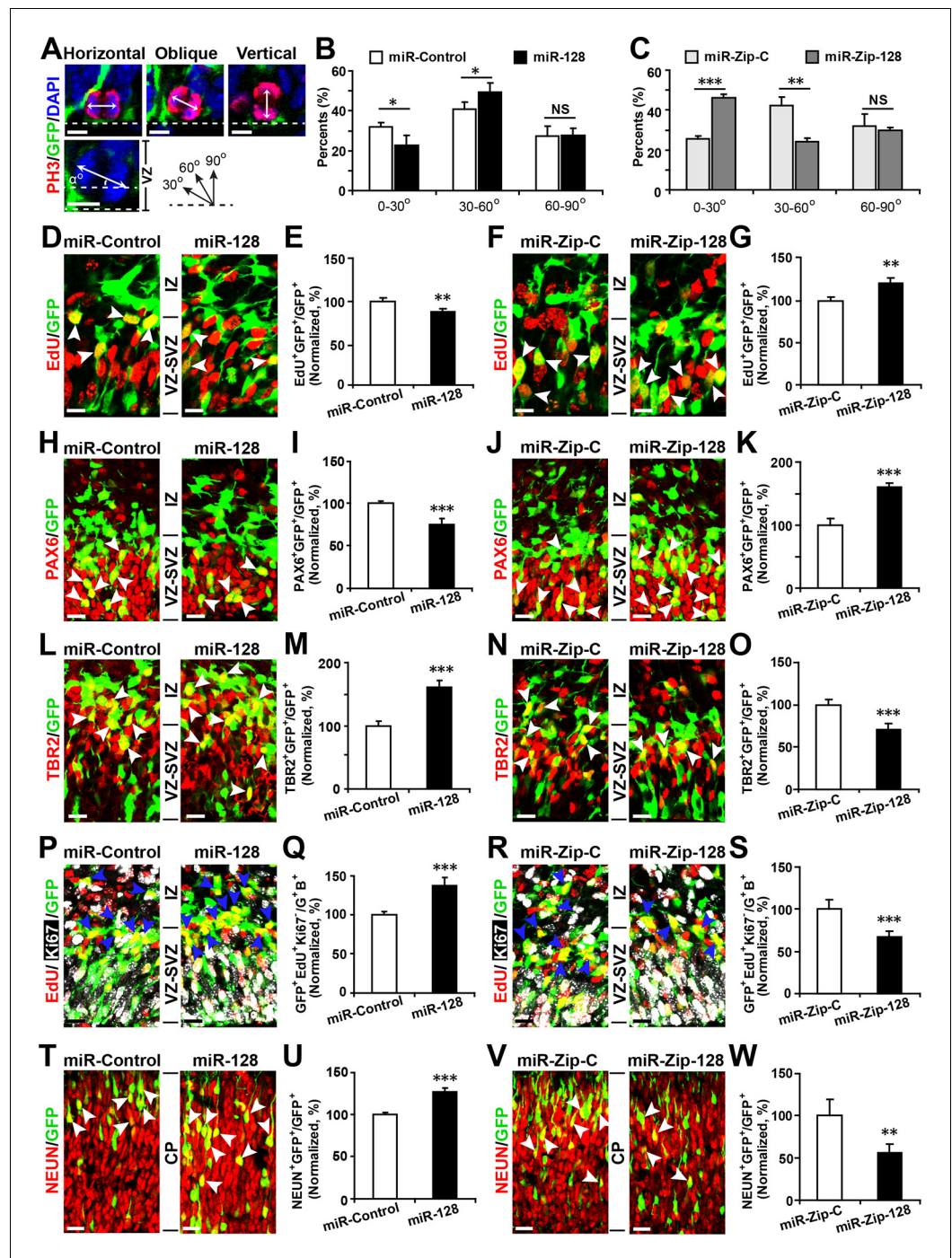DOI: 10.7554/eLife.11324.011

Figure 3. miR-128 regulates the proliferation and differentiation of NPCs in vivo. (**A-C**) miR-128 regulates the symmetric division of apical progenitors in the VZ/SVZ. Mouse embryos were electroporated at E13.5 with the indicated plasmids and sacrificed at E14.5. The nuclei of mitotic cells were labeled using antibodies against PH3. The orientation of the mitotic spindle relative to the ventricular surface was determined and categorized into horizontal (0–30°), oblique (30–60°), or vertical (60–90°) as pictured. Scale bars, 5 μm. (**A**). Percentage of GFP and PH3 double-positive cells with the indicated mitotic spindle orientation following miR-128 overexpression (**B**) and miR-128 knockdown (**C**). (**D-G**) miR-128 regulates the proliferation of apical progenitors in the VZ/SVZ. Mouse embryos were electroporated at E13.5 with the indicated constructs. Twenty-four hours post-electroporation, dividing cells were marked by EdU pulse-labeling for 2 hr and sacrificed. The arrowheads indicate EdU⁺GFP⁺ cells. Scale bars, 10 μm. Quantification of the number of GFP-EdU double-positive cells relative to the number of GFP-positive cells (**E, G**). (**H–K**) Ectopic expression of miR-128 decreases apical progenitors, while that of miR-Zip-128

Figure 3 continued on next page

Figure 3 continued

increases apical progenitors. Mouse embryos were electroporated at E13.5 with the indicated constructs and sacrificed at E14.5. Brain sections were immunostained with antibodies against PAX6. The arrowheads indicate PAX6$^+$GFP$^+$ cells. Scale bars, 10 μm. Quantification of the number of GFP-PAX6 double-positive cells relative to the number of GFP-positive cells (**I, K**). (**L–O**) Ectopic expression of miR-128 increases basal progenitors, while that of miR-Zip-128 decreases basal progenitors. Mouse embryos were electroporated at E13.5 with the indicated constructs and sacrificed at E14.5. Brain sections were immunostained with antibodies against TBR2. The arrowheads indicate TBR2$^+$GFP$^+$ cells. Scale bars, 10 μm. Quantification of the number of GFP-TBR2 double-positive cells relative to the number of GFP-positive cells (**M, O**). (**P-S**) miR-128 promotes cell cycle exit, and miR-Zip-128 inhibits cell cycle exit. Mouse embryos were electroporated at E13.5 with the indicated constructs. Twenty-four hours post-electroporation, dividing cells were marked by EdU pulse-labeling for 24 hr and sacrificed. The brain sections were immunostained with antibodies against Ki67. The blue arrowheads indicate GFP$^+$EdU$^+$Ki67$^-$ cells that had exited the cell cycle. Scale bars, 10 μm. Quantification of the number of GFP-EdU double-positive, Ki67-negative cells relative to the number of GFP-BrdU double-positive cells (**Q, S**). (**T-W**) miR-128 promotes the differentiation of NPCs in vivo. Mouse embryos were electroporated at E13.5 with the indicated constructs and sacrificed at E17.5. Brain slices were immunostained for NEUN. Arrowheads indicate NEUN$^+$GFP$^+$ cells. Scale bars, 10 μm. Quantification of the number of GFP-NEUN double-positive cells relative to the number of GFP-positive cells (**U, W**). More than 1500 GFP-positive cells were counted for each condition. At least three sets of independent experiments were performed. The values represent the mean ± s.d. (n = 3). Student's *t*-test, differences were considered significant at ***p<0.001, **p<0.01, and *p<0.05.
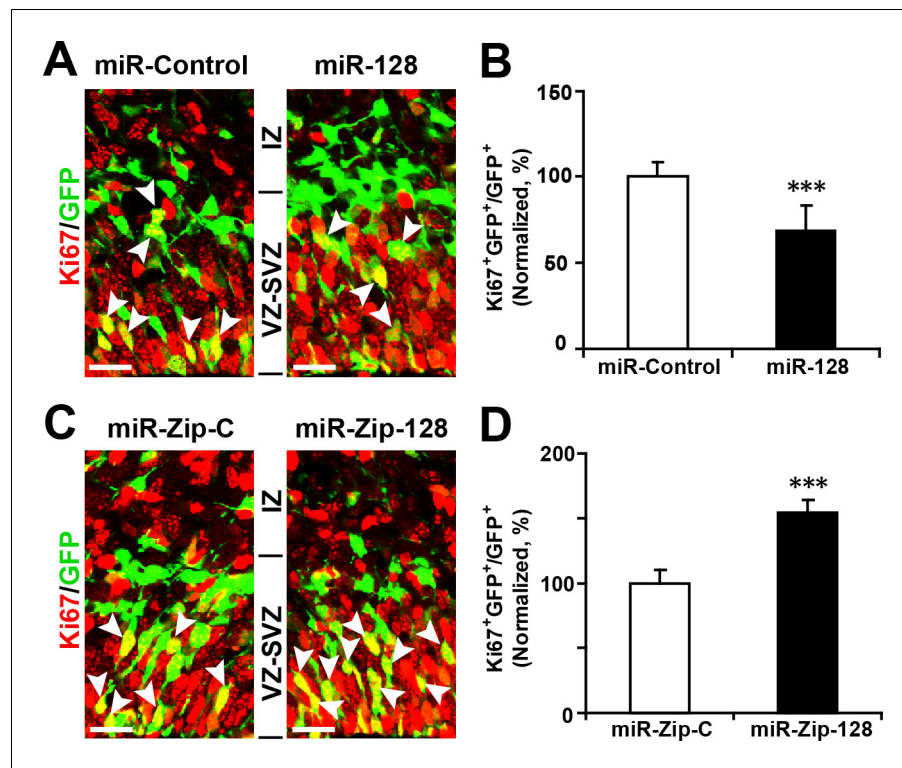DOI: 10.7554/eLife.11324.012

Figure 3—figure supplement 1. Ectopic expression of miR-128 decreases proliferation, while that of miR-Zip-128 increases proliferation in vivo. (A-D) Mouse embryos were electroporated at E13.5 with the indicated constructs and sacrificed at E14.5. Brain sections were immunostained with antibodies against Ki67. The arrowheads indicate Ki67$^+$GFP$^+$ cells. Scale bars, 10 µm. Quantification of the number of GFP-Ki67 double-positive cells relative to the number of GFP-positive cells (B, D). More than 1500 GFP-positive cells were counted for each condition. At least three sets of independent experiments were performed. The values represent the mean ± s.d. (n = 3). Student's *t*-test, differences were considered significant at ***p<0.001.
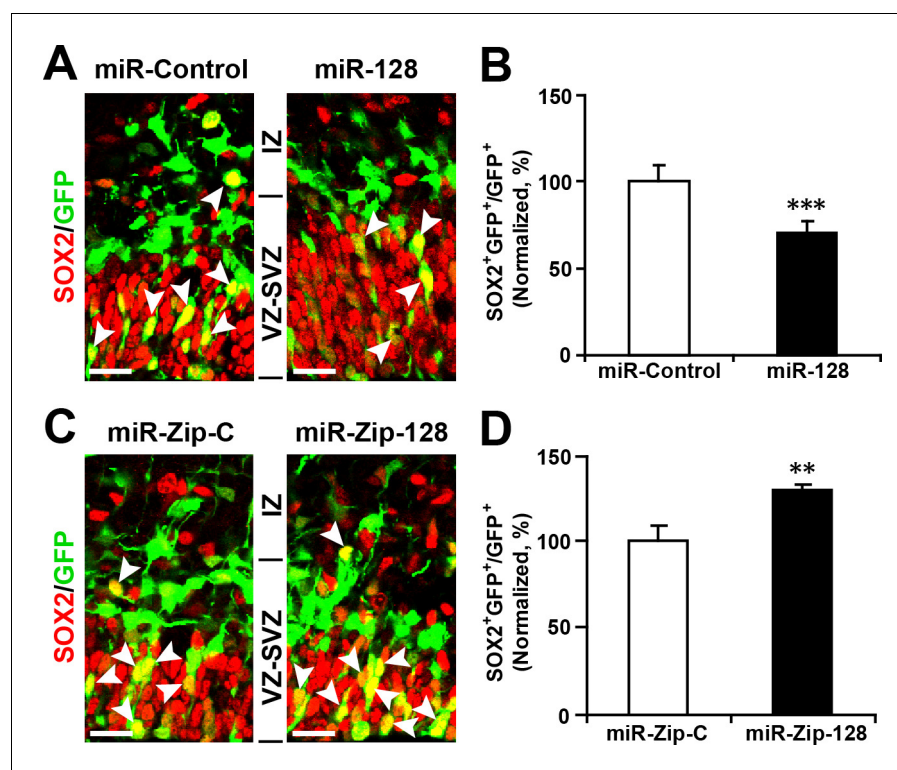DOI: 10.7554/eLife.11324.013

Figure 3—figure supplement 2. Ectopic expression of miR-128 decreases apical progenitors, while that of miR-Zip-128 increases apical progenitors. (A-D) Mouse embryos were electroporated at E13.5 with the indicated constructs and sacrificed at E14.5. Brain sections were immunostained with antibodies against SOX2. The arrowheads indicate SOX2$^+$GFP$^+$ cells. Scale bars, 10 µm. Quantification of the number of GFP-SOX2 double-positive cells relative to the number of GFP-positive cells (B, D). More than 1500 GFP-positive cells were counted for each condition. At least three sets of independent experiments were performed. The values represent the mean ± s.d. (n = 3). Student's *t*-test, differences were considered significant at ***p<0.001 and **p<0.01.
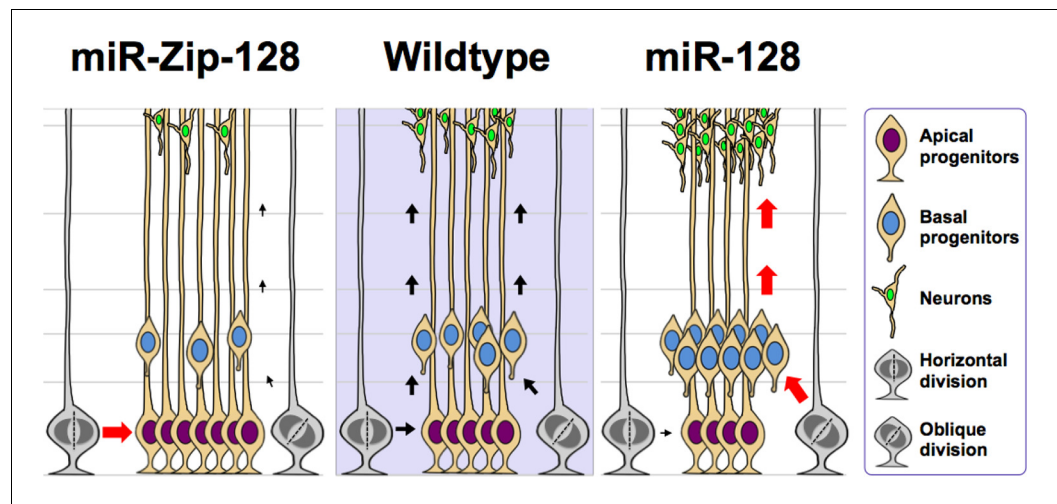DOI: 10.7554/eLife.11324.014

Figure 3—figure supplement 3. Model of the miR-128 in vivo phenotype. miR-128 overexpression in embryonic neural stem cells leads to two phenotypes that when combined together, ultimately results in amplified neurogenesis. First, an increase in the asymmetric cell division of apical progenitors occurs, which results in a relatively higher number of basal progenitors and a lower number of apical progenitors. Second, an increase in cell cycle exit occurs in the expanded basal progenitor pool, which leads to a greater number of neurons. miR-128 knockdown results in the opposite phenotypes, namely an increase in the symmetric cell division of apical progenitors, resulting in a relatively higher number of apical progenitors and a lower number of basal progenitors. In addition, the basal progenitors do not exit the cell cycle as readily, ultimately leading to a smaller number of neurons.
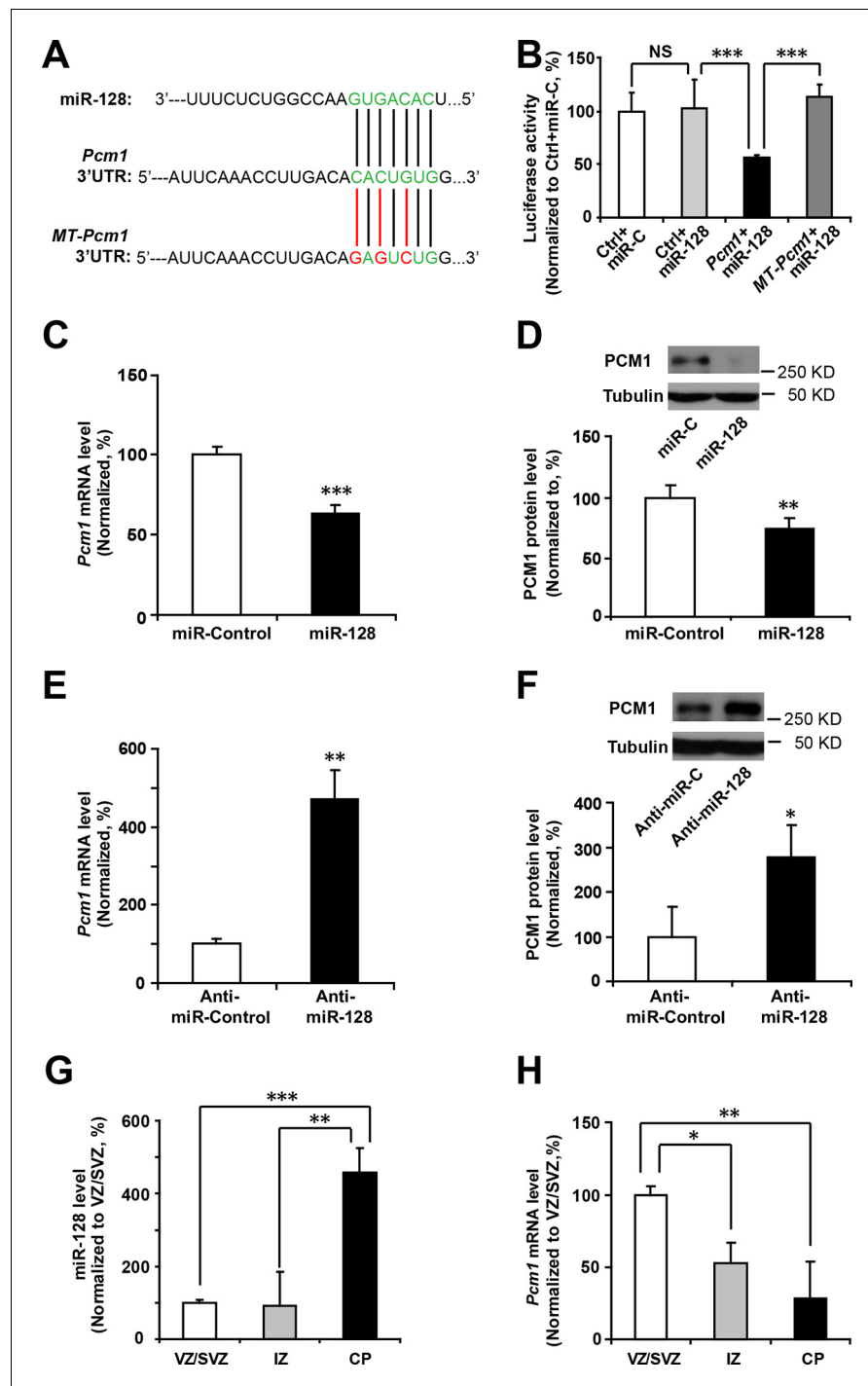
DOI: 10.7554/eLife.11324.015

Figure 4. miR-128 regulates PCM1 expression in NPCs. (**A**) TargetScan analysis identified a miR-128 target site in the mouse *Pcm1* 3'-UTR region (highlighted in green). The mutant PCM1 is shown, with the seed binding sites highlighted in red. (**B**) PCM1 luciferase activity is suppressed by miR-128. HEK293T cells were co-transfected with miR-128 and the 3'-UTR of *Pcm1* containing either the miRNA binding site (WT) or mutant (MT) versions of the *Pcm1* seed binding sites for 2 days. The cells were harvested and lysed, and a luciferase activity assay was then performed. miR-128-mediated suppression of PCM1 luciferase activity was relieved upon mutation of the *Pcm1* seed binding sites. (**C,D**) miR-128 overexpression in NPCs led to reduced endogenous *Pcm1* mRNA levels, as determined by qPCR (**C**), and PCM1 protein expression, as demonstrated via densitometry analysis of western blots (**D**). (**E,F**) anti-miR-128 leads to increased endogenous *Pcm1* mRNA levels, as demonstrated by qPCR (**E**), and protein expression of PCM1 (**F**). (**G,H**) LCM was used to isolate RNA from three specific cortical layers of E14.5

Figure 4 continued on next page

Figure 4 continued

embryonic brains: the VZ/SVZ, IZ, and CP. qPCR quantification of miR-128 levels (**G**) and *Pcm1* mRNA levels (**H**). At least three sets of independent experiments were performed. The values represent the mean ± s.d. (n = 3). Student's *t*-test, differences were considered significant at ***p<0.001, **p<0.01, and *p<0.05 for all panels in the figure. ANOVA, differences were considered significant at ***p<0.001 and **p<0.01.

DOI: 10.7554/eLife.11324.016

The following source data is available for figure 4:

Source data 1. Gene Ontology (GO) of the miR-128 target gene list.
DOI: 10.7554/eLife.11324.017
Source data 2. Relative expression of 53 predicted miR-128 targets upon overexpression of miR-128 in NPCs.
DOI: 10.7554/eLife.11324.018
Source data 3. Relative expression of miR-128 targets upon downregulation of miR-128 in NPCs using miR-Zip-128.
DOI: 10.7554/eLife.11324.019
Source data 4. List of qPCR primers.
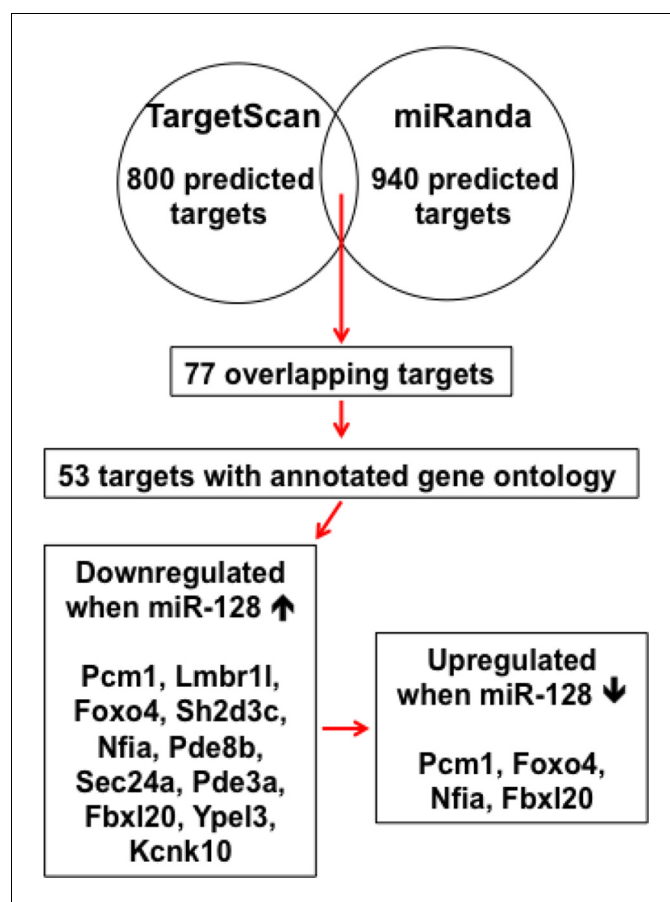DOI: 10.7554/eLife.11324.020

Figure 4—figure supplement 1. Schematic diagram outlines rationale of gene selection process. Two widely used in silico microRNA target prediction databases (TargetScan and miRanda) predicted 800 and 940 potential targets of miR-128 respectively. Among the 77 overlapping targets only 53 were annotated to have known biological function and only 11 out of the 53 genes exhibited consistent reduction in mRNA levels upon miR-128 overexpression in cultured mouse NPCs and were further tested for reciprocal upregulation when miR-128 was inhibited. Lastly, upon miR-128 inhibition in NPCs, only *Pcm1, Nfia, Foxo4,* and *Fbxl20* were consistently upregulated.
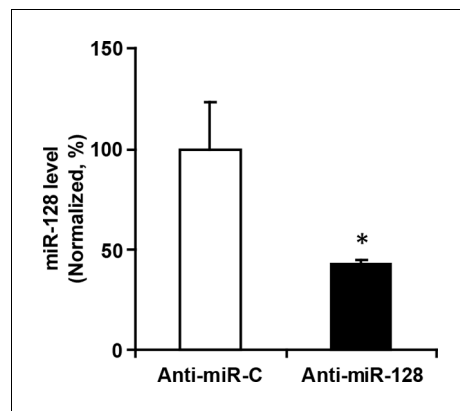
DOI: 10.7554/eLife.11324.021

Figure 4—figure supplement 2. miR-128 inhibitor knockdown efficiency. qPCR quantification of miR-128 levels in NPCs following transfection with 2 µg miR-128 inhibitor (anti-miR-128) compared to the scramble control (anti-miR-control). The values represent the mean ± s.d. (n = 3). Student's t-test, differences were considered significant at *p<0.05.
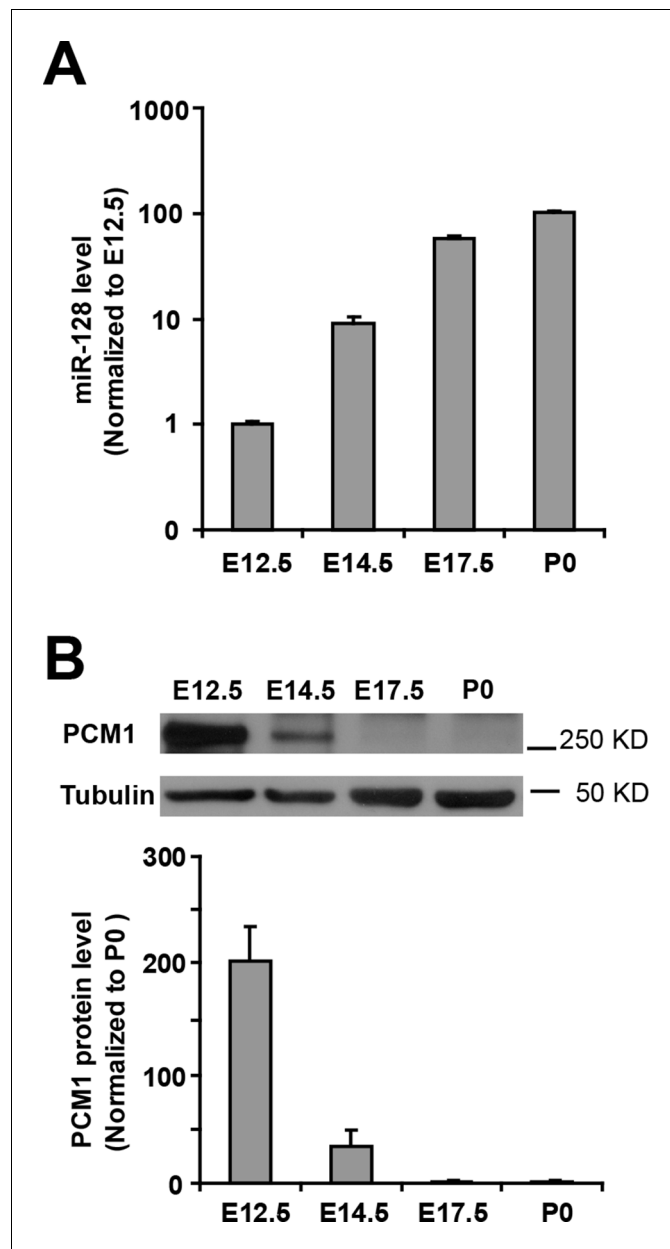DOI: 10.7554/eLife.11324.022

Figure 4—figure supplement 3. Inverse relationship between the temporal expression patterns of miR-128 and PCM1. (**A**) Real-time PCR analyses of miR-128 from brain tissues at various developmental stages. miR-128 expression was measured and normalized to that of U6 and is shown relative to the E12.5 expression level. The values represent the mean ± s.d. (n = 3). (**B**) Western blot of PCM1 expression in brain lysates prepared at various developmental stages with densitometry analysis. The values represent the mean ± s.d. (n = 3). Student's *t*-test, differences were considered significant at *p<0.05.
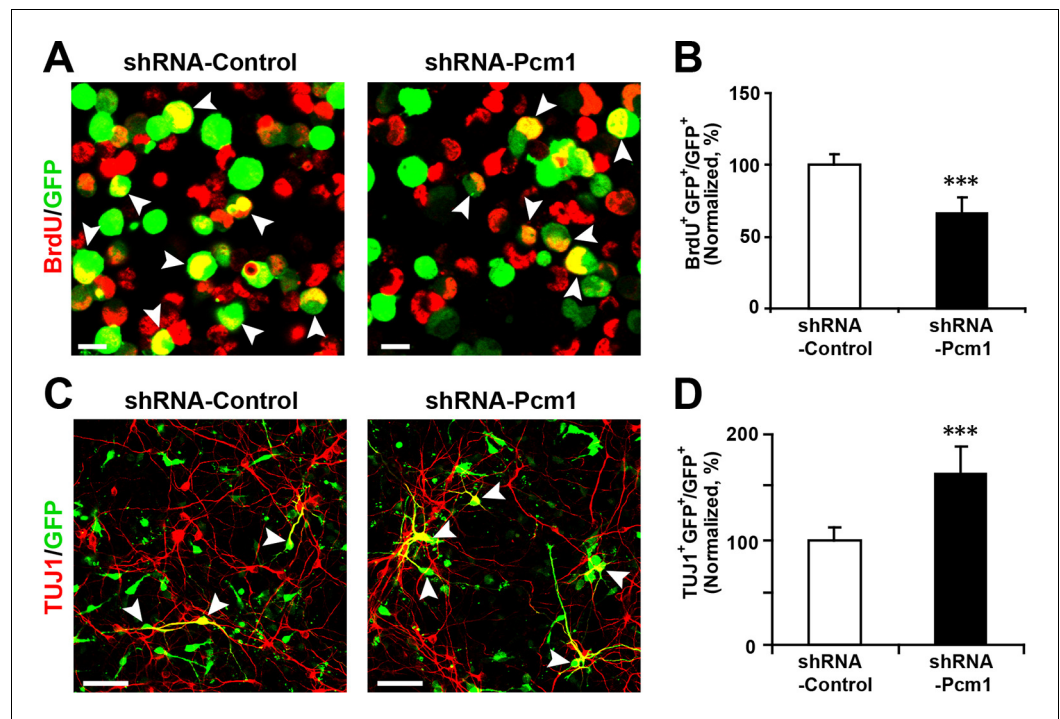DOI: 10.7554/eLife.11324.023

Figure 5. PCM1 knockdown decreases NPC neurogenesis. (**A,B**) PCM1 knockdown in NPCs decreases neural proliferation. NPCs were electroporated with a plasmid expressing PCM1 shRNA or with a control vector and pulse-labeled with BrdU for 6 hr. NPCs were immunostained with an antibody against BrdU. The arrowheads indicate BrdU and GFP double-positive cells. Scale bars, 10 μm. Quantification of the number of GFP-BrdU double-positive cells relative to the total number of GFP-positive cells (**B**). (**C,D**) PCM1 knockdown in NPCs increases neurogenesis. NPCs were electroporated with a plasmid expressing PCM1 shRNA or with a control vector and then immunostained with antibodies against TUJ1. The arrowheads indicate TUJ1$^+$GFP$^+$ cells. Scale bars, 50 μm. Quantification of the number of GFP-TUJ1 double-positive cells relative to the number of GFP-positive cells (**D**). More than 1500 GFP-positive cells were counted for each condition. At least three sets of independent experiments were performed. The values represent the mean ± s.d. (n = 3). Student's *t*-test, differences were considered significant at ***p<0.001.
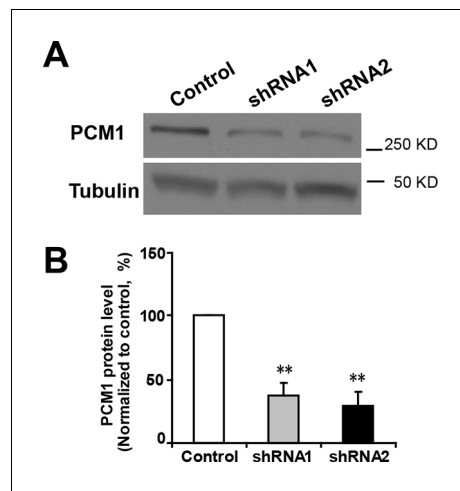DOI: 10.7554/eLife.11324.024

Figure 5—figure supplement 1. Efficient knockdown of PCM1. (A) PCM1 knockdown in N2A cells demonstrated by western blots. (B) Densitometry analysis of western blots presented in (A). PCM1 shRNA2 was used for further proliferation and neurogenesis analysis in NPCs. At least three sets of independent experiments were performed. The values represent the mean ± s.d. (n = 3). Student's *t*-test, differences were considered significant at **p<0.01.
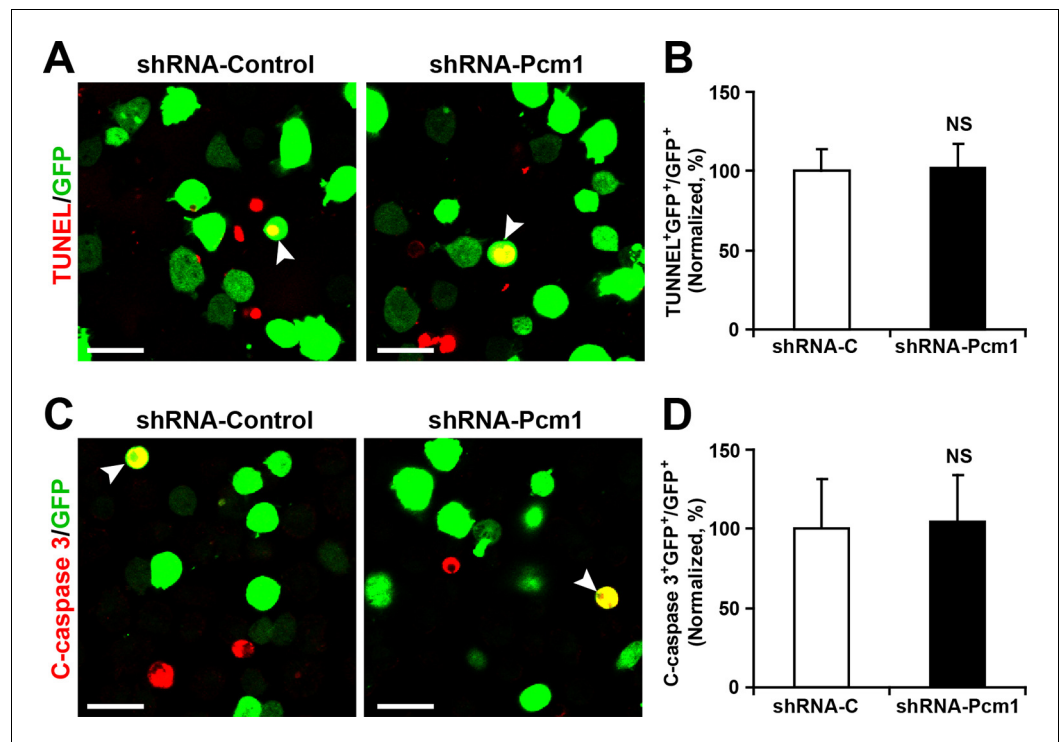DOI: 10.7554/eLife.11324.025

Figure 5—figure supplement 2. PCM1 knockdown in NPCs did not trigger apoptotic cell death. (**A,B**) Ectopic expression of PCM1 shRNA does not affect TUNEL staining. Quantification of the number of GFP-TUNEL double-positive cells relative to the total number of GFP-positive cells (**B**). (**C,D**) Ectopic expression of PCM1 shRNA does not affect cleaved caspase-3 (C-caspase 3) staining. Scale bars, 20 μm. Quantification of the number of GFP-C-caspase 3 double-positive cells relative to the total number of GFP-positive cells (**D**). More than 1500 GFP-positive cells were counted for each condition. At least three sets of independent experiments were performed. The values represent the mean ± s.d. (n = 3). Student's *t*-test, differences were considered significant at *$p<0.05$.
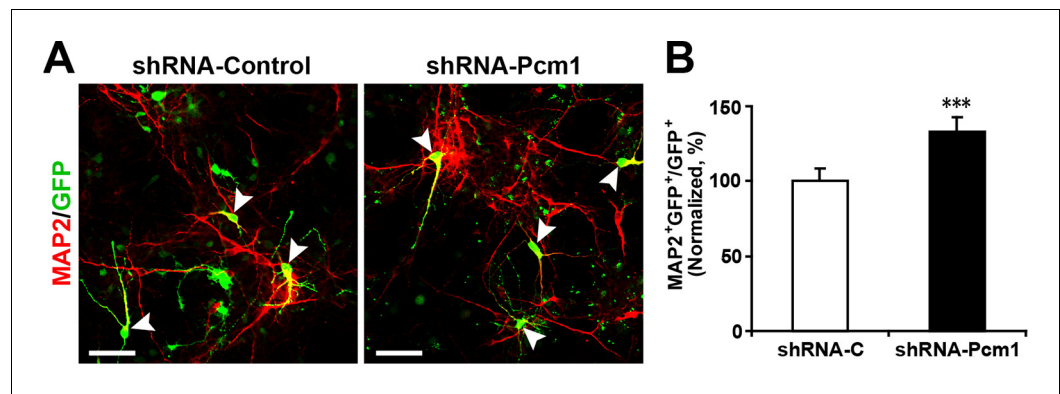DOI: 10.7554/eLife.11324.026

Figure 5—figure supplement 3. PCM1 knockdown in NPCs increases neurogenesis. (A-,B) NPCs were electroporated with a plasmid expressing PCM1 shRNA or with a control vector and then immunostained with antibodies against MAP2. The arrowheads indicate MAP2$^+$GFP$^+$ cells. Scale bars, 50 μm. Quantification of the number of GFP-MAP2 double-positive cells relative to the number of GFP-positive cells (B). More than 1500 GFP-positive cells were counted for each condition. At least three sets of independent experiments were performed. The values represent the mean ± s.d. (n = 3). Student's t-test, differences were considered significant at ***$p<0.001$.
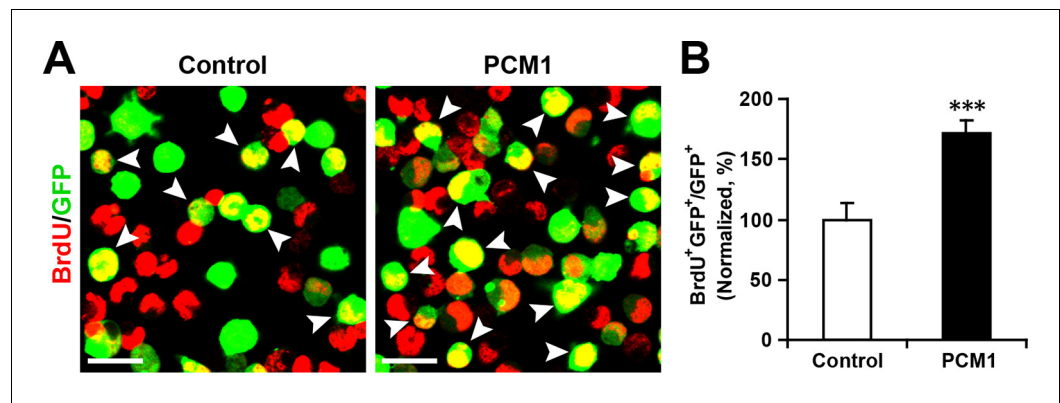
Figure 5—figure supplement 4. Overexpression of PCM1 increases NPC proliferation. (**A,B**) Overexpression of PCM1 increases NPC proliferation. NPCs were electroporated with a PCM1 overexpression construct or a control vector and pulse-labeled with BrdU for 6 hr. NPCs were immunostained with an antibody against BrdU. The arrowheads indicate BrdU and GFP double-positive cells. Scale bars, 10 μm. Quantification of the number of GFP-BrdU double-positive cells relative to the total number of GFP-positive cells (**B**). More than 1500 GFP-positive cells were counted for each condition. At least three sets of independent experiments were performed. The values represent the mean ± s.d. (n = 3). Student's *t*-test, differences were considered significant at ***p<0.001.
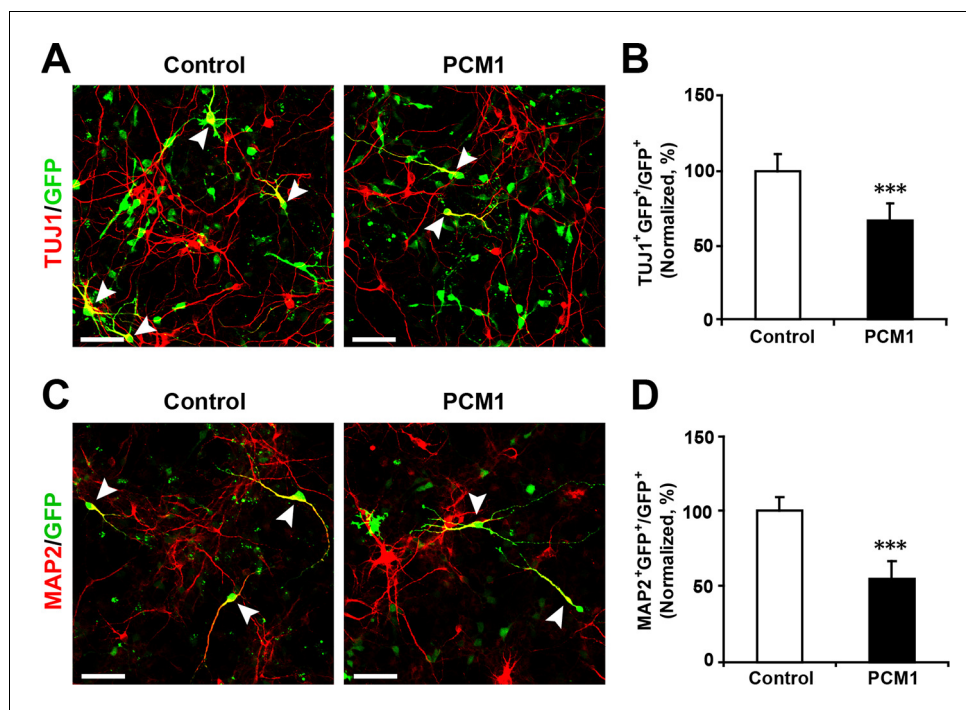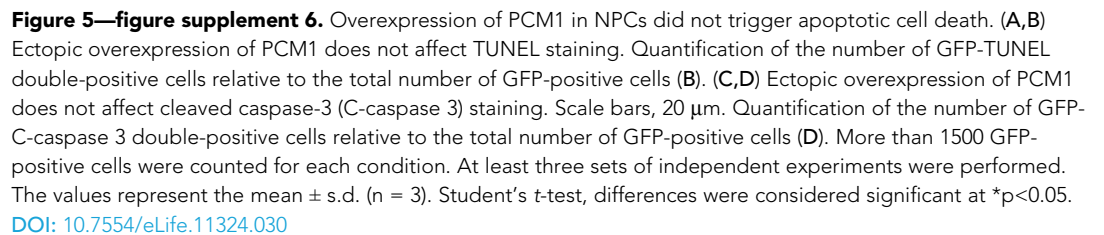DOI: 10.7554/eLife.11324.028

Figure 5—figure supplement 5. Overexpression of PCM1 decreases NPC neuronal differentiation. (A,B) Ectopic expression of PCM1 decreases TUJ1 staining. NPCs were electroporated with a PCM1 overexpression construct or a control vector and immunostained with antibodies against TUJ1. The arrowheads indicate TUJ1$^+$GFP$^+$ cells. Scale bars, 50 μm. Quantification of the number of GFP-TUJ1 double-positive cells relative to the number of GFP-positive cells (B). (C,D) Ectopic expression of PCM1 decreases MAP2 staining. NPCs were electroporated with the indicated plasmids and immunostained with antibodies against MAP2. The arrowheads indicate MAP2$^+$GFP$^+$ cells. Scale bars, 50 μm. Quantification of the number of GFP-MAP2 double-positive cells relative to the number of GFP-positive cells (D). More than 1500 GFP-positive cells were counted for each condition. At least three sets of independent experiments were performed. The values represent the mean ± s.d. (n = 3). Student's t-test, differences were considered significant at ***p<0.001.
DOI: 10.7554/eLife.11324.029

Figure 5—figure supplement 6. Overexpression of PCM1 in NPCs did not trigger apoptotic cell death. (A,B) Ectopic overexpression of PCM1 does not affect TUNEL staining. Quantification of the number of GFP-TUNEL double-positive cells relative to the total number of GFP-positive cells (B). (C,D) Ectopic overexpression of PCM1 does not affect cleaved caspase-3 (C-caspase 3) staining. Scale bars, 20 μm. Quantification of the number of GFP-C-caspase 3 double-positive cells relative to the total number of GFP-positive cells (D). More than 1500 GFP-positive cells were counted for each condition. At least three sets of independent experiments were performed. The values represent the mean ± s.d. (n = 3). Student's *t*-test, differences were considered significant at *$p < 0.05$. DOI: 10.7554/eLife.11324.030
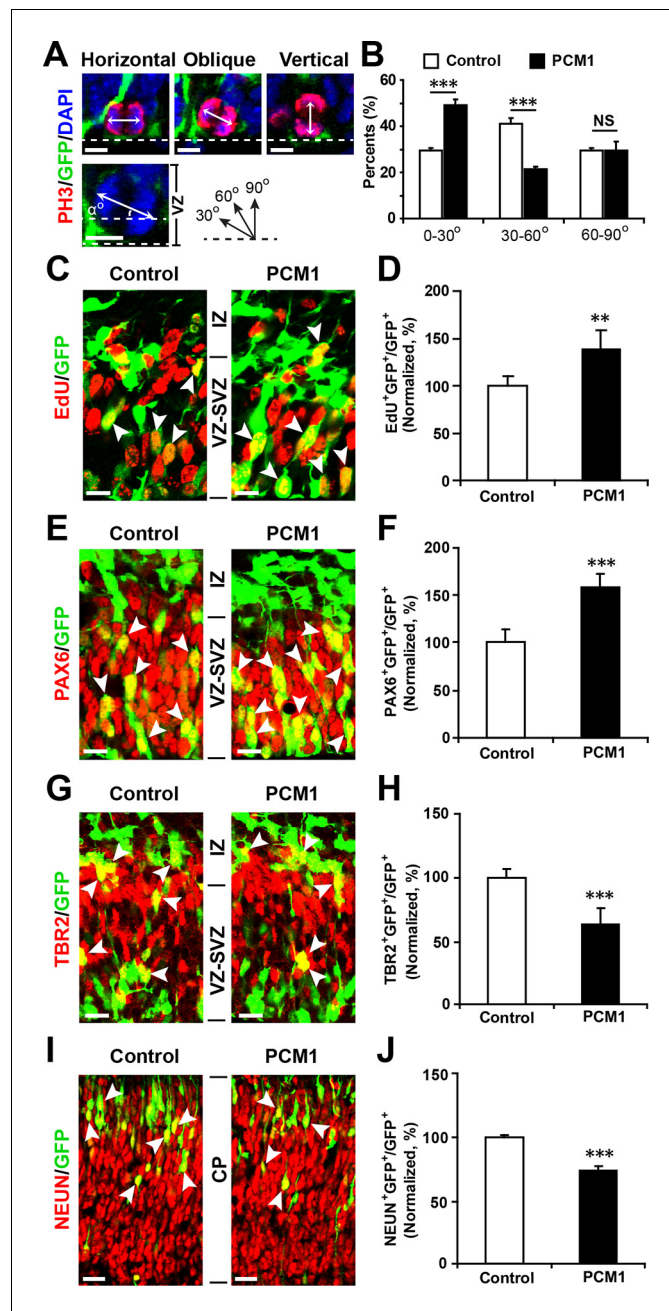
Figure 5—figure supplement 7. PCM1 regulates NPC proliferation and differentiation in vivo. (**A,B**) PCM1 regulates the symmetric division of apical progenitors in the VZ/SVZ. Mouse embryos were electroporated at E13.5 with the indicated plasmids and sacrificed at E14.5. The nuclei of mitotic cells were labeled using antibodies against PH3. The orientation of the mitotic spindle relative to the ventricular surface was determined and categorized into horizontal (0–30°), oblique (30–60°), or vertical (60–90°) as pictured. Scale bars, 5 μm (**A**). Percentage of GFP and PH3 double-positive cells with the indicated mitotic spindle orientation following PCM1 overexpression (**B**). (**C,D**) Overexpression of PCM1 increases NPC proliferation in vivo compared to vector-only control treatment. Mouse embryos were electroporated at E13.5 with the indicated constructs. Twenty-four hours post-electroporation, dividing cells were marked by EdU pulse-labeling for 2 hr and sacrificed. The arrowheads indicate EdU$^+$GFP$^+$ cells. Scale bars, 10 μm. Quantification of the number of GFP-EdU double-positive cells relative to the number of GFP-positive cells (**D**). (**E,F**) Overexpression of PCM1 increases apical progenitors compared to vector-only control treatment. Mouse embryos were electroporated at E13.5 with the indicated constructs and sacrificed at E14.5. Brain sections were immunostained with antibodies against PAX6. The arrowheads indicate PAX6$^+$GFP$^+$ cells. Scale bars, 10 μm. Quantification of the number of GFP-PAX6 double-

Figure 5—figure supplement 7 continued on next page

Figure 5—figure supplement 7 continued

positive cells relative to the number of GFP-positive cells (**F**). (**G,H**) Overexpression of PCM1 decreases the number of basal progenitors compared to vector-only control treatment. Mouse embryos were electroporated at E13.5 with the indicated constructs and sacrificed at E14.5. Brain sections were immunostained with antibodies against TBR2. The arrowheads indicate TBR2$^+$GFP$^+$ cells. Scale bars, 10 µm. Quantification of the number of GFP-TBR2 double-positive cells relative to the number of GFP-positive cells (**H**). (**I,J**) Overexpression of PCM1 decreases neurogenesis compared to vector-only control treatment. Mouse embryos were electroporated at E13.5 with the indicated constructs and sacrificed at E17.5. Brain slices were immunostained for NEUN. Arrowheads indicate NEUN$^+$GFP$^+$ cells. Scale bars, 10 µm. Quantification of the number of GFP-NEUN double-positive cells relative to the number of GFP-positive cells (**J**). More than 1500 GFP-positive cells were counted for each condition. At least three sets of independent experiments were performed. The values represent the mean ± s.d. (n = 3). Student's *t*-test, differences were considered significant at ***$p < 0.001$.
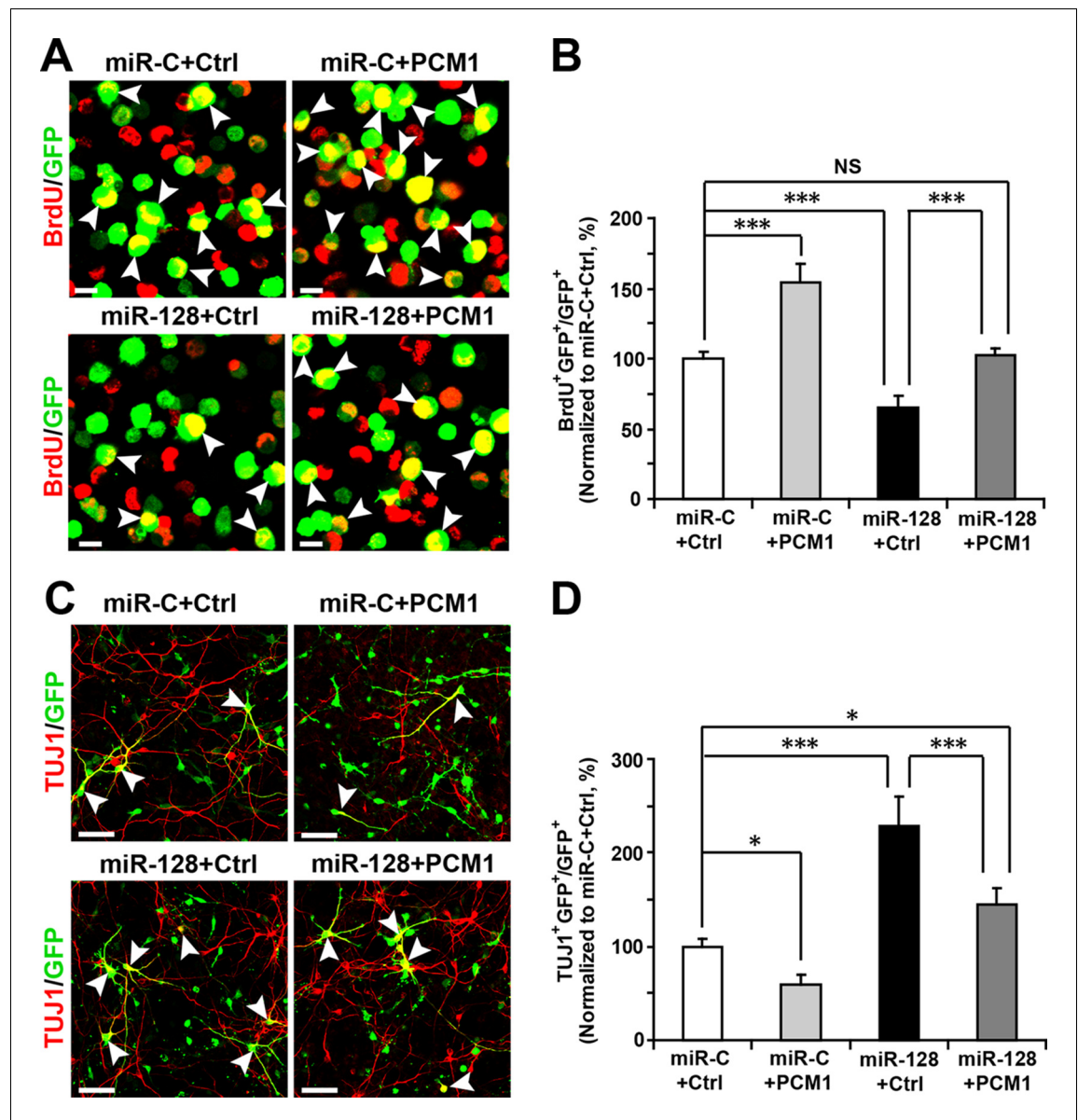DOI: 10.7554/eLife.11324.031

Figure 6. PCM1 is a functional target of miR-128 in vitro. (**A,B**) PCM1 antagonizes the effects of miR-128 on NPC proliferation in vitro. NPCs were electroporated with a miRNA control vector or with miR-128. Either a PCM1 expression construct or vector only control was co-electroporated in miR-128-expressing NPCs to examine the rescue effect of PCM1 in these cells. The cells were pulse-labeled with BrdU for 6 hr, and a proliferation assay was performed by immunostaining for BrdU (**A**). Scale bars, 10 μm. (**B**) Quantification of BrdU and GFP double-positive cells, demonstrating that PCM1 overexpression in the miR-128 cells rescued the reduced proliferation in the miR-128-expressing cells. (**C,D**) miR-128 antagonizes the function of PCM1 in neurogenesis in vitro. A neuronal differentiation assay was performed by immunostaining for TUJ1. The arrowheads indicate cells that are double-positive for TUJ1 and GFP (**C**). Scale bars, 50 μm. (**D**) Quantification of TUJ1 and GFP double-positive cells, demonstrating that PCM1 overexpression in the miR-128-expressing cells reverses the increased neurogenesis phenotype of the miR-128-expressing cells. More than 2000 GFP-positive cells were counted for each condition. At least three sets of independent experiments were performed. The values represent the mean ± s.d. (n = 3). ANOVA, differences were considered significant at ***p<0.001, **p<0.01 and *p<0.05.
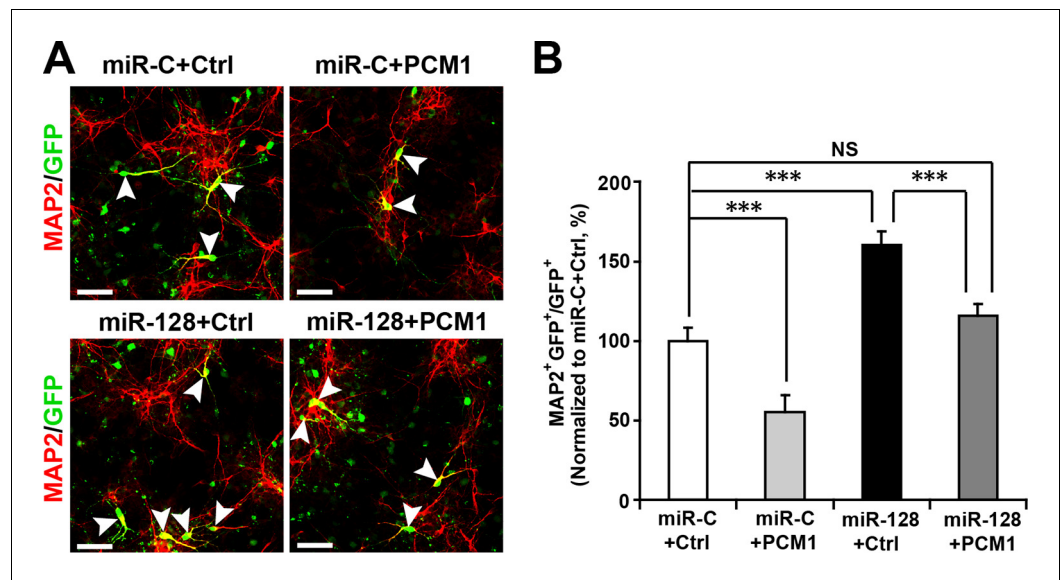DOI: 10.7554/eLife.11324.032

Figure 6—figure supplement 1. PCM1 is a functional target of miR-128 in vitro. NPCs were electroporated with a miRNA control vector or with miR-128. Either a PCM1 expression construct or vector only control was co-electroporated in miR-128-expressing NPCs to examine the rescue effect of PCM1 in these cells. A neuronal differentiation assay was performed by immunostaining for MAP2. The arrowheads indicate cells that are double-positive for MAP2 and GFP (A). Scale bars, 50 μm. (B) Quantification of MAP2 and GFP double-positive cells, demonstrating that PCM1 overexpression in the miR-128-expressing cells rescues the enhanced neurogenesis phenotype of the miR-128-expressing cells. More than 2000 GFP-positive cells were counted for each condition. At least three sets of independent experiments were performed. The values represent the mean ± s.d. (n = 3). ANOVA, differences were considered significant at ***$p<0.001$ and **$p<0.01$.
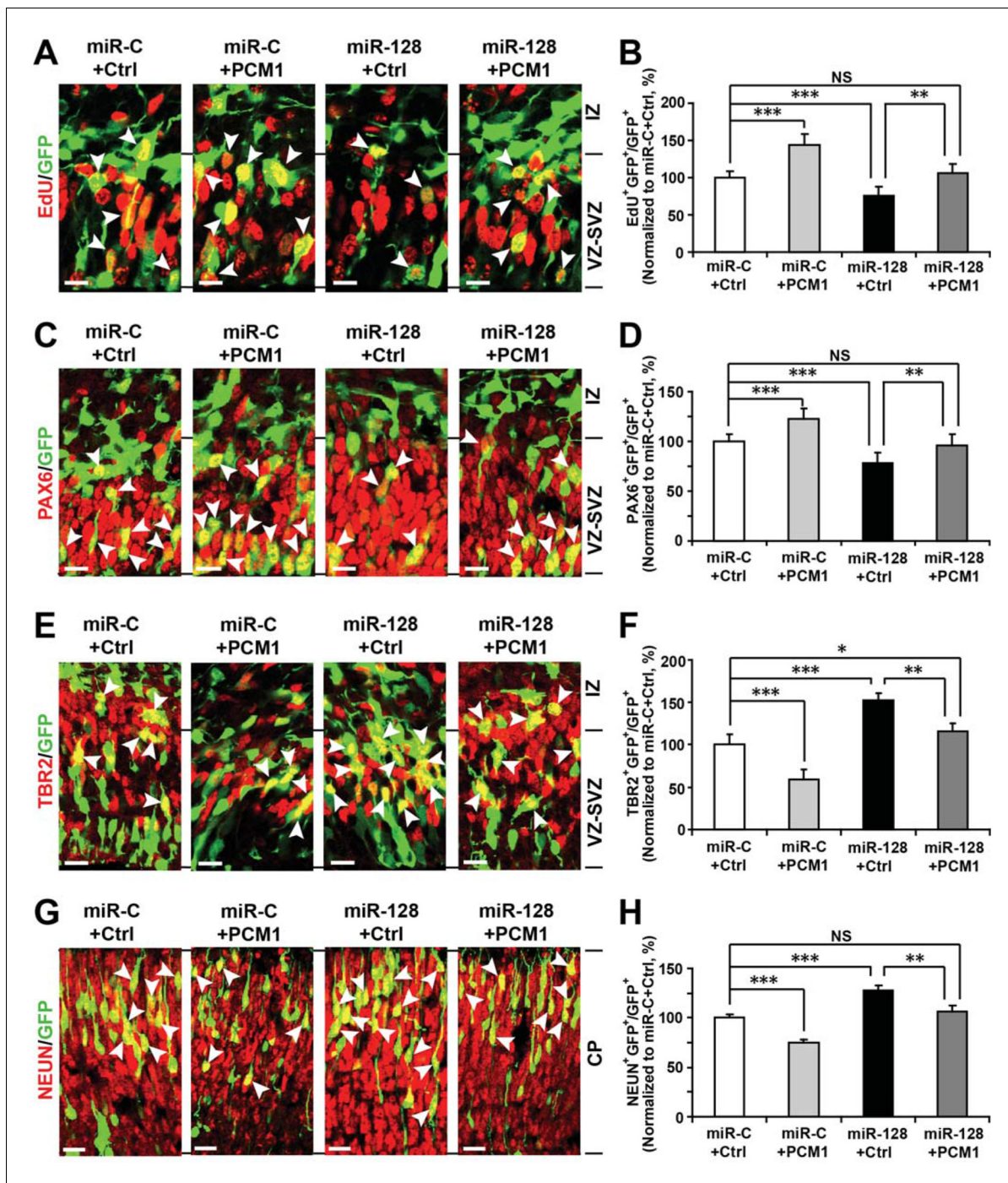DOI: 10.7554/eLife.11324.033

Figure 7. PCM1 is a downstream target of miR-128 during NPC proliferation and differentiation in vivo. (A,B) PCM1 antagonizes the effects of miR-128 on NPC proliferation in vivo. Mouse embryos were electroporated at E13.5 with a miRNA control vector or with miR-128. Either a PCM1 expression construct or vector only control was co-electroporated in miR-128-expressing NPCs to examine the rescue effect of PCM1 in these cells. Twenty-four hours post-electroporation, dividing cells were marked by EdU pulse-labeling for 2 hr and sacrificed. The arrowheads indicate EdU+GFP+ cells. Scale bars, 10 µm. Quantification of the number of GFP-EdU double-positive cells relative to the number of GFP-positive cells (B). (C,D) PCM1 overexpression rescues the miR-128-mediated decrease in the number of apical progenitors. Mouse embryos were electroporated at E13.5 with the indicated constructs and sacrificed at E14.5. Brain sections were immunostained with antibodies against PAX6. The arrowheads indicate PAX6+GFP+ cells. Scale bars, 10 µm. Quantification of the number of GFP-PAX6 double-positive cells relative to the number of GFP-positive cells (D). (E,F) PCM1 overexpression rescues the miR-128-mediated increase in the number of basal progenitors. Mouse embryos were electroporated at E13.5 with the indicated constructs and sacrificed at E14.5. Brain sections were immunostained with antibodies against TBR2. The arrowheads indicate TBR2+GFP+ cells. Scale bars, 10 µm. Quantification of the number of GFP-TBR2 double-positive cells relative to the number of GFP-positive cells (F). (G,H) PCM1

Figure 7 continued on next page

Figure 7 continued

overexpression rescues the miR-128-mediated increase in neurogenesis. Mouse embryos were electroporated at E13.5 with the indicated constructs and sacrificed at E17.5. Brain slices were immunostained for NEUN. Arrowheads indicate NEUN$^+$GFP$^+$ cells. Scale bars, 10 μm. Quantification of the number of GFP-NEUN double-positive cells relative to the number of GFP-positive cells (**H**). More than 1500 GFP-positive cells were counted for each condition. At least three sets of independent experiments were performed. The values represent the mean ± s.d. (n = 3). ANOVA, differences were considered significant at ***p<0.001 and **p<0.01.